

Production of Wind Tunnel Testing Models with use of Rapid Prototyping Methods

R. ADELNIA¹, S. DANESHMAND², S. AGHANAJAFI³
Mechanical Group, Majlesi Azad University
Isfahan
IRAN

Abstract: In a time when “better, faster, cheaper” are the words to live by, new technologies must be employed to try and live up to these axioms. In this spirit, a study has been undertaken to determine the suitability of models constructed using rapid prototyping (RP) methods for use in subsonic, transonic, wind tunnel testing. This study was conducted to determine if the level of development in rapid prototyping materials and processes is adequate for constructing models, and if these models meet the structural requirements of subsonic, transonic, testing while still having the high fidelity required to produce accurate aerodynamic data. The findings from this initial study indicated that the aerodynamic database obtained from RP models showed good agreement with data obtained from the machined Aluminum counterpart.

Key -Words: Rapid prototyping, Wind tunnel testing, Construction costs, Wind Tunnel Models, Aerodynamic Characteristics, stereolithography

1 Introduction

This study provides the necessary data to compare the aerodynamic characteristics of an RP model to that of a standard Aluminum machined model. It was conducted to determine if certain criteria can be satisfactorily met in order to produce an adequate assessment of vehicle aerodynamic characteristics[1]. These pertinent questions or criteria were as follows: (1) could RP methods be used to produce a detailed scale model within required dimensional tolerances?

(2) Did the available RP materials have the mechanical characteristics, strength, and elongation properties required to survive wind tunnel testing at subsonic and transonic speeds and still produce accurate data?

(3) Which RP process or processes and materials produce the best results?

(4) What are the costs and time requirements for the various RP methods as compared to a standard machined metal model?

RP models constructed using four methods and six materials were compared to a machined metal model [2]. The RP processes were fused deposition method (FDM) using materials of both acrylonitrile butadiene styrene (ABS) plastic and Poly Ether Ether Keytone (PEEK) stereolithography (SLA)

with a photopolymer resin of STL-5170. Selective laser sintering (SLS) with glass reinforced nylon as a material [3] and laminated object method (LOM) using both plastic reinforced with glass fibers and “paper” [4]. Aluminum (Al) was chosen as the material for the machined metal model. An aluminum model, while not as preferred as a steel model, costs less and requires less time to construct, thus providing a more conservative baseline model. This study focused on a small aspect of wind tunnel testing determining the static stability aerodynamic characteristics of a vehicle relevant to preliminary vehicle configuration design. While some of the RP methods or processes had reached a mature level of development, such as SLA, LOM using “paper” and FDM using ABS plastic. The other three RP methods tested were SLA, SLS, and FDM-ABS [5].

2 Rapid Prototyping (RP) Technique

At present some of the RP methods or processes had reached a mature level of development, such as SLA, LOM using “paper,” and FDM using ABS plastic, while others still were in the development phase. The fused deposition method (FDM) involves the layering of molten beaded ABS plastic material via a movable nozzle in 0.25 millimeter thick layers. Stereolithography uses a vat of a photopolymer

¹ - PhD candidate

² - PhD candidate

³ - Associate Professor

epoxy resin which solidifies when hit by a UV laser. The laser solidifies each layer as the tray is lowered. This continues until the part is complete are shown in figure 1.

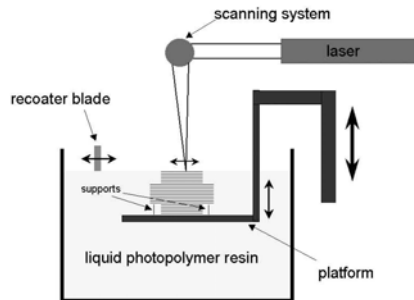


Fig. 1- The stereolithography method (SLA)

The ABS material is supplied in rolls of thin ABS line resembling weed trimmer line. The material is heated and extruded through a nozzle similar to that of a hot glue gun. The plastic is deposited in rows and layered forming the part from numerically controlled (NC) data [6]. Stereolithography method (SLA) uses a vat of a photopolymer epoxy resin which solidifies when hit by a UV laser. The laser solidifies each layer as the tray is lowered. This continues until the part is complete [7]. Selective laser sintering method (SLS) uses a laser to fuse or sinter powdered glass and nylon particles or granules in layers which are fused on top of each other as with the other processes [8]. Some of wind tunnel testing models are produced with RP methods are shown in figure 2 [9].



Fig. 2- Wing-body models tested (left to right), aluminum, FDM-ABS, SLA, and SLS

3 Geometry

The wing-body-tail configuration is shown in fig. 2. This configuration would indicate possible deflections in the wings or tail due to loads and whether the manufacturing accuracy of the airfoil sections would adversely affect the aerodynamic data that resulted during testing and will the model

be able to withstand the starting, stopping and operating loads in a blowdown wind tunnel [10].

Computer Aided design (CAD) file be used for aluminum model design and fabrication is used for RP model. The reference dimensions for this configuration are as follows:

$$S_{ref}=56.02\text{cm}^2 \quad L_{ref}=226.61\text{mm}$$

$$X_{MRP}=158.63\text{mm aft of nose}$$

Each of the RP models was constructed as a single part. The nose section was separated from the core and a 19-mm hole was drilled and reamed through the center of the body for placement of the aluminum balance adapter, which was then epoxied and pinned into place. The nose was attached to the core body with two screws which were attached through the nose to the balance adapter. Figure 3 shows a finished FDM model, its nose removed and an aluminum balance adapter as used in the models [11]. The material properties of SLA, FDM-ABS, SLS and Aluminum are shown in table 1 and 2.

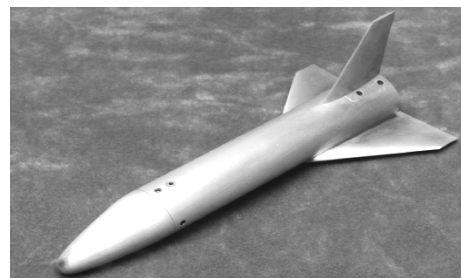


Fig. 3- Wing-body-tail configuration

Table 1- Material properties of SLA, FDM-ABS, and SLS

| Property | Units | SLA SL5170 | SLS Protoform | FDM - ABS |
|---------------------|---------|------------|---------------|-----------|
| Tensile strength | Mpa | 59.24 | 48.91 | 34.45 |
| Tensile modulus | Mpa | 3961.75 | 2811.12 | 2480.40 |
| Elongation at break | Percent | 12 | 6 | 50 |
| Flexural strength | Mpa | 107.48 | - | 65.45 |
| Flexural modulus | Mpa | 2955.81 | 4306.25 | 2618.20 |
| Impact strength | N | 32.12 | 66.92 | 107.08 |
| Hardness | Shore D | 45 | - | 10 |

Table 2 - Material properties of aluminum

| Property | AL 2024-T4 | AL 5086-H32 |
|------------------------|------------|-------------|
| Yield strength (Mpa) | 275.60 | 192.92 |
| Tensile strength (Mpa) | 427.18 | 275.60 |

4 Wind Tunnel Testing

Four models are tested in wind tunnel. Three of the four models were constructed using rapid prototyping methods while the fourth acted as a control, being a standard machine tooled metal model. Ability to produce accurate airfoil sections, and to determine the material property effects

related to the bending of the wing and tail under loading, are parameters which would be tested. All models were tested at angle of attack ranges from -4 degrees to +16 degrees at zero sideslip and at angle of sideslip ranges from -8 to +8 degrees at 6 degrees angle of attack. The reference aerodynamic axis system and reference parameters for the baseline study are shown in figure 4.

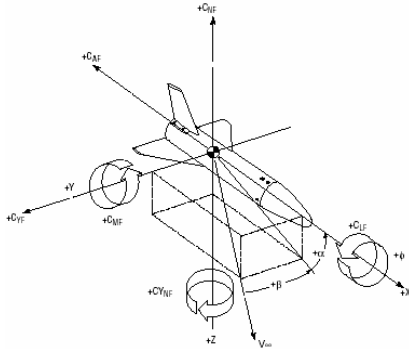


Fig. 4- Wing-body aerodynamic axis system

For all phases of the baseline study representative Mach numbers of 0.3, 0.8, 1.05 and 1.2 are presented in this report. Table 3 shows the relation between Mach number, dynamic pressure, and Reynolds number for wind tunnel operating [12].

Table 3- Wind tunnel operating conditions

| Mach Number | Reynolds Number | Dynamic Pressure |
|-------------|-----------------------|------------------|
| 0.3 | $91.80 \times 10^6/m$ | 8.96 KPa |
| 0.8 | 18.03 | 44.58 |
| 1.05 | 20 | 58.43 |
| 1.2 | 20.32 | 63.7 |

Coefficients of normal force, axial force, pitching moment, and lift over drag are shown at each of these Mach numbers. Only data for much number 1.2 are shown in figure 5 through figure 8 for this study. The study showed that between Mach numbers of 0.3 to 1.2 the longitudinal aerodynamic data or data in the pitch plane showed very good agreement between the metal model and SLA model up to about 12 degrees angle-of-attack when it started to diverge due to assumed SLA model surface bending under higher loading. The initial SLS data for all the coefficients do not accurately represent the process because the model was a different configuration due to post-processing problems. The second SLS model tested showed much better agreement with the data trends from the other models, but was not as good as the FDM and SLA. The greatest difference in the aerodynamic

data between the models at Mach numbers of 0.3 to 1.2 was in total axial force. In general, it can be said that all the RP model longitudinal aerodynamic data at subsonic Mach numbers showed a slight divergence at higher angles-of attack when compared to the metal model data. At transonic Mach numbers the majority of the configurations started diverging at about 10 to 12 degrees angle-of-attack due to the higher loads encountered by the models.

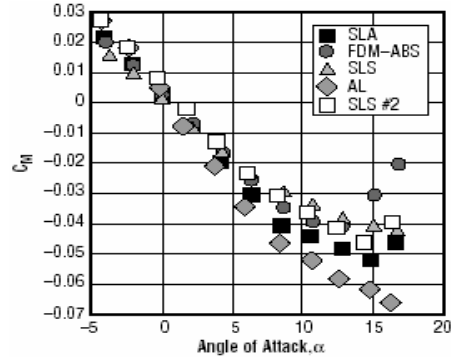


Fig.5- Comparison of pitching moment coefficient at Mach 1.2

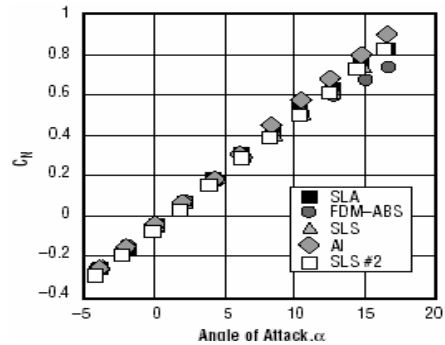


Fig.6- Comparison of normal force coefficient at Mach 1.2

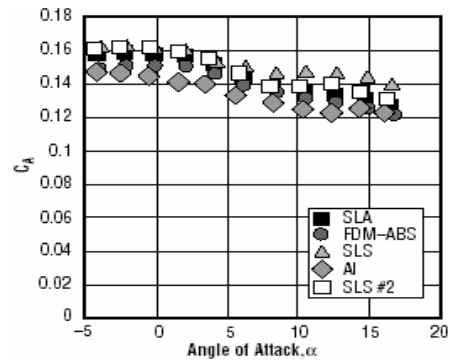


Fig.7- Comparison of axial force coefficient at Mach 1.2

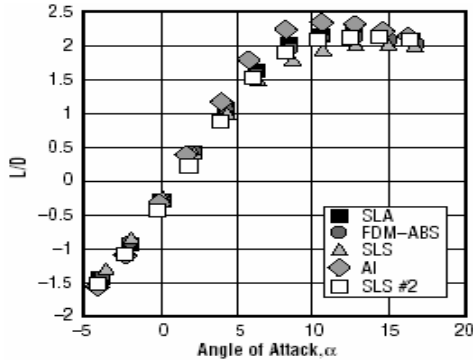


Fig.8- Comparison of lift over drag at Mach 1.2

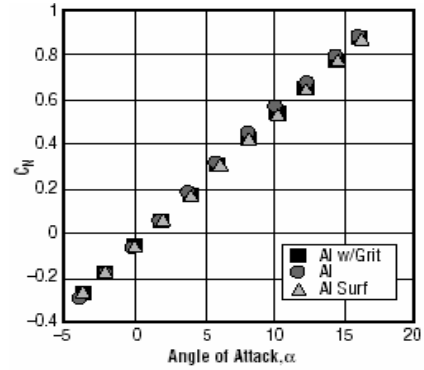


Fig.10- Comparison of normal force coefficient At Mach 1.2

5 Surface Finish

The effects of surface finish and grit on the aerodynamic characteristics of the models were determined. The RP models did not have as smooth a finish as did the aluminum model, so runs were made to determine if the difference in these surface finishes would affect the aerodynamic characteristics. A rough surface finish was simulated on the aluminum model by covering the full model in a layer of silicon carbide particles called “grit.” This grit would “rough” up the surface. The effect of grit on the model was also determined. Grit is used to trip the boundary layer over the model to simulate a higher Reynolds number than the actual wind tunnel Reynolds number. The effect of these changes is shown in figures 9 through 12. In these graphs it can be seen that surface finish does have an effect on the aerodynamic characteristics. The application of grit had little effect on the aerodynamic characteristics except for axial force and its derivative coefficients.

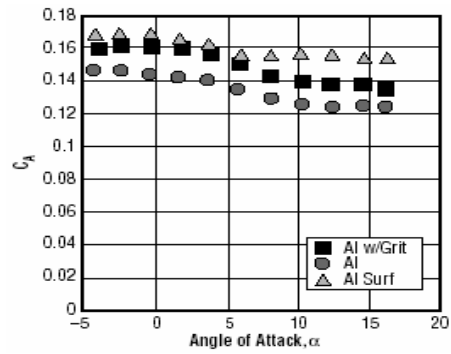


Fig.11- Comparison of axial force coefficient At Mach 1.2

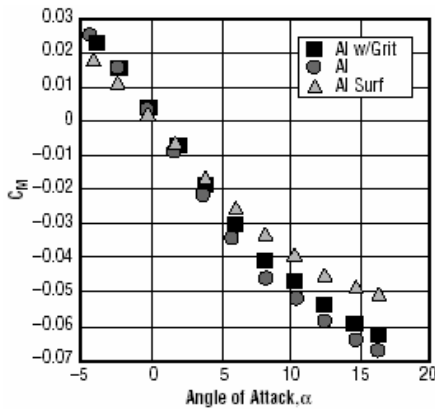


Fig.9- Comparison of pitching coefficient At Mach 1.2. moment

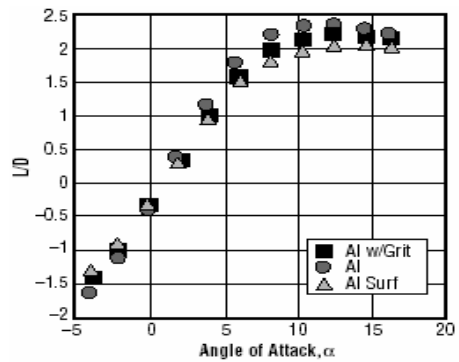


Fig.12- Comparison of lift over drag at Mach 1.2

6 Cost and Time

The cost and time requirements for the various RP models and the metal model are shown in table 4 time and cost consumption in metal models has about five times the RP models.

Table 4- Wind tunnel model time and cost summary

| Model Cost and Time | SLA | FDM -ABS | LOM | SLS | AI |
|---------------------|--------|----------|--------|--------|---------|
| RP Model | \$1200 | \$1000 | \$900 | \$1400 | |
| Conversion | 2000 | 2000 | 2000 | 2000 | |
| Balance-Adapter | 100 | 100 | 100 | 100 | |
| Total Cost | 3300 | 3100 | 3000 | 3500 | \$15000 |
| Time | 2-3 Ws | 2-3 Ws | 2-3 Ws | 2-3 Ws | 3 ½ Ms |

Ws= Weeks, Ms= Months

7 Accuracy

Difference between dimensions and the model’s balance adapter rolling has the most effect on aerodynamics coefficient difference of two models. The contours of the models used in this test were measured at two wing sections, vehicle stations, tail sections, and the XY and XZ planes. A comparison of model dimensions is shown in table 5.

Table 5- Model dimensions compared to theoretical

| | AL | SLS | SLA | FDM | SLS2 |
|----------|-------|-------|-------|-------|-------|
| Wing L1 | 0.246 | 0.497 | 0.170 | 0.220 | 0.231 |
| Wing L2 | 0.109 | 0.398 | 0.124 | 0.165 | 0.403 |
| Wing R1 | 0.106 | 0.259 | 0.134 | 0.071 | 0.480 |
| Wing R2 | 0.137 | 0.220 | 0.152 | 0.109 | 0.378 |
| Body 1 | 0.177 | 0.109 | 0.071 | 0.365 | 0.116 |
| Body 2 | 0.048 | 0.304 | 0.139 | 0.304 | 0.139 |
| Tail 1 | 0.078 | 0.259 | 0.111 | 0.078 | 0.238 |
| Tail 2 | 0.050 | 0.254 | 0.073 | 0.071 | 0.129 |
| XY plane | .030 | 0.078 | 0.759 | 0.165 | 0.236 |
| XZ plane | 0.076 | 0.447 | 0.637 | 1.386 | 0.609 |

Two sectional cuts were made on each wing, left and right; two on the body; two on the vertical tail, and one cut in the XY and XZ planes. This shows a representation of the maximum discrepancy in model dimensions relative to the baseline CAD model used to construct all the models at each given station. The RP model’s balance adapter was rolled approximately 2 degrees starboard wing down, while the metal model’s balance adapter was rolled approximately 0.5 degree port wing down. The effect of the balance adapter roll on the normal force and side force aerodynamic coefficients is shown in table 6 if a C_N of 1.0 and a C_Y of 0.0 are assumed.

Table 6- Effect of balance adapter roll on aerodynamic coefficients

| Roll Angle | C_N | C_Y |
|------------|--------|--------|
| 0.5° | 0.9999 | 0.0087 |
| 1 | 0.9998 | 0.0175 |
| 1.5 | 0.9997 | 0.0262 |
| 2 | 0.9994 | 0.0349 |
| 2.5 | 0.9990 | 0.0436 |

8 Conclusions

Rapid prototyping methods have been shown to be feasible in their limited direct application to wind tunnel testing for producing preliminary aerodynamic databases. Cost savings and model design/fabrication time reductions of over a factor of 5 have been realized for RP techniques as compared to current standard model design/fabrication practices.

- The differences between the configurations data can be attributed to multiple factors such as surface finish, structural deflection, and tolerances on the fabrication of the models when they are “grown.”
- Wind tunnel models constructed using rapid prototyping methods and materials can be used in subsonic and transonic wind tunnel testing for initial baseline aerodynamic database development.
- SLA was shown to be the best RP process with satisfactory results for a majority of the test conditions.

References:

[1] Chua, C.K., Leong, K.F. and Lim, C.S. (2003), Rapid Prototyping: Principles and Application, 2nd ed., World Scientific, New Jersey, NJ.

[2] Bae, S.C., Gerber, H., Kim, T.S, Lee, J. H., Wieneke-Toutaoui, B. (2001): Rapid Prototyping for the Presentation of Large Size Products. Proc URapid 2001, Amsterdam

[3] Pandey, P.M., Thrimurthullu, K., Reddy, N.V. (2004) Optimal Part Deposition Orientation in FDM using Multi-Criteria GA, International Journal of Production Research, 42(19), pp. 4069-4089.

[4] Onuh, S. O. 2001. Rapid prototyping integrated systems. Rapid Prototyping Journal 7, no. 4:220-223.

[5] Pandey, P.M., Reddy N.V., Dhande, S.G. (2003) Slicing Procedures in Layered Manufacturing: A Review, Rapid Prototyping Journal, 9(5), pp. 274-288.

[6] Thrimurthullu, K., Pandey, P.M., Reddy, N.V. (2004) Part Deposition Orientation in Fused Deposition Modeling, International Journal of Machine Tools and Manufacture, 2004, 44, pp. 585-594.

[7] “Stereolithography Process”, online image 2002, <http://www.cadcamnet.com> . 6 Aug. 2003.

[8] Wohlers, Terry T.,” Rapid Prototyping & Tooling State of the Industry”, Annual Worldwide Progress Report. Fort Collins, Colorado, (2000).

[9] COOPER, K. Rapid Prototyping Technology. New York, Marcel Dekker, 2001. Pp.13-137

- [10] Springer A., Cooper K., "Application of Rapid Prototyping Methods to High Speed Wind Tunnel Testing", proceedings of 86th Semiannual Meeting Supersonic Tunnel Association, October (1996).
- [11] Springer A. and Cooper K., "Comparing the Aerodynamic Characteristics of Wind Tunnel Models Produced by Rapid Prototyping and Conventional Methods", AIAA 97-2222, 15th AIAA Applied Aerodynamics Conference, June (1997).
- [12] Springer, A.; Cooper, K.; and Roberts, F. "Application of Rapid Prototyping Models to Transonic Wind Tunnel Testing", AIAA 97-0988, 35th Aerospace Sciences Meeting. January 1997.